Lee *et al.*
Journal of Analytical Science and Technology (2023) 14:34
https://doi.org/10.1186/s40543-023-00400-6

Journal of Analytical Science and Technology

RESEARCH ARTICLE

Open Access

Liquid chromatography-tandem mass spectrometry for pharmacokinetics evaluation of AZD5305, a selective PARP1 inhibitor, in mice

Gi Ju Lee[1†], Jin Woo Kim[1†], Hae-In Choi[1], Jin Young Choi[1], Kwan Hyung Cho[2] and Tae-Sung Koo[1*]

Abstract

Poly (ADP-ribose) polymerase (PARP) inhibitors that are effective against ovarian and breast cancers with breast cancer susceptibility gene (BRCA) mutations have undesirable side effects, such as hematological toxicity. AZD5305, a selective PARP1 inhibitor currently in Phase 1/2 clinical trials, may avoid the side effects caused by PARP2. However, the in vivo pharmacokinetic characteristics of AZD5305 and its bioanalytical methods are unknown. Therefore, a method based on liquid chromatography with tandem mass spectroscopy (LC–MS/MS) was developed and validated to quantify AZD5305 in plasma of mice. Optimal chromatographic separation in terms of peak intensity and symmetry was acquired using a 4-μm Polar-RP 80 Å (2.0 × 150 mm) column with ammonium acetate (5 mM) in distilled water–acetonitrile (50:50, v/v). The retention times of AZD5305 and internal standard (IS; olaparib) were 1.82 min and 1.99 min, respectively. Detection was carried out via triple quadrupole mass spectrometry in positive ion mode employing multiple reaction monitoring transitions at m/z 407.0 → 376.0 for AZD5305 and m/z 435.0 → 281.2 for the IS. The LC–MS/MS method was linear in the range 1–1000 ng/mL with a correlation coefficient ≥ 0.990 and showed acceptable values of major parameters including accuracy, precision, and recovery. Additionally, AZD5305 showed high stability under various conditions. The in vivo and in vitro pharmacokinetics of AZD5305 were successfully characterized by employing the validated LC–MS/MS method. A high level of drug exposure and linear pharmacokinetics were observed after intravenous (IV) bolus and oral administration (PO) of AZD5305 at 0.1–1 mg/kg and 0.1–3 mg/kg, respectively. The bioavailability was close to 100%, and the metabolic stability of AZD5305 in hepatic microsomes of mice and humans was very high. These results may contribute to the improvement of PARP inhibitors that are used to treat malignancies originating from BRCA mutations.

Keywords AZD5305, Poly (ADP-ribose) polymerase inhibitor, Liquid chromatography-tandem mass spectrometry, Pharmacokinetics

[†]Gi Ju Lee and Jin Woo Kim have contributed equally to this work.

*Correspondence:
Tae-Sung Koo
kootae@cnu.ac.kr
Full list of author information is available at the end of the article

Introduction

Poly (ADP-ribose) polymerase (PARP) and proteins encoded for by the breast cancer susceptibility gene 1/2 (BRCA1/2) are crucial for DNA repair via base excision and homologous recombination (HR) in humans (Dziadkowiec et al. 2016). However, BRCA mutations result in a reduced ability to repair damaged DNA, leading to the development of cancer and other genetic changes. In 2016, the International Cancer Center reported that 50–60% elderly female patients with breast cancer had BRCA1/2 mutations (Armstrong et al. 2019). Single-strand breaks accumulate in the presence of a PARP inhibitor (Dziadkowiec et al. 2016), which causes increased replication errors and double-strand breaks (DSBs), eventually leading to apoptosis of cells with BRCA mutations (Lee et al. 2014). In normal cells, the DSBs induced by PARP inhibitors are repaired by HR; however, in cancers caused by BRCA mutations, HR does not occur, resulting in synthetic lethality (Dziadkowiec et al. 2016). This mechanism selectively targets cancer cells with BRCA mutations and shows minimal toxicity (Chen 2011).

Drugs, such as olaparib, rucaparib, talazoparib, and niraparib, have shown efficacy against breast and ovarian cancers with BRCA mutations (Mateo et al. 2019). However, all approved PARP inhibitors have undesirable side effects such as hematological toxicity (Bruin et al. 2022; Illuzzi et al. 2021). Synthetic lethality occurs when only PARP1 is inhibited in the presence of a BRCA mutation, suggesting that PARP2 does not have anticancer effects and causes hematological toxicity (Johannes et al. 2021; Murai et al. 2012). Although PARP2 inhibition is not required for high efficacy, all approved PARP inhibitors inhibit both PARP1 and PARP2 (Illuzzi et al. 2021). Therefore, AstraZeneca, the developer of olaparib, is currently developing AZD5305, a selective PARP1 inhibitor in Phase 1/2 clinical trials (Clinical Trials.gov US 2023). Unlike existing PARP inhibitors, AZD5305 has approximately 500-times higher selectivity for PARP1 than for PARP2; therefore, it may reduce the side effects caused by PARP2 inhibition. Notably, AZD5305 has demonstrated high selectivity to PARP1 in preclinical models, significantly reducing hematological toxicity (Illuzzi et al. 2021). Furthermore, the study revealed that AZD5305 inhibited tumor growth in BRCA mutant xenograft models, indicating its effectiveness as a targeted anticancer agent. Additionally limited information on plasma concentrations was reported together, including patterns of unbound plasma concentrations after administration to mice and the AUC value of unbound concentrations in rats co-administered with carboplatin (Illuzzi et al. 2021).

Despite promising preclinical results, bioanalytical methods for AZD5305 are currently not available, and limited pharmacokinetic information has been reported (Illuzzi et al. 2021; Langelier et al. 2023). Therefore, we established an LC–MS/MS assay for AZD5305 in mouse plasma and investigated the in vivo and in vitro pharmacokinetics of AZD5305 in mice. Our results can provide insights into the pharmacological properties of AZD5305 and aid in developing more effective PARP inhibitors for treating cancers associated with BRCA mutations.

Materials and methods

Materials

AZD5305 ($C_{22}H_{26}N_6O_2$; MW, 406.48; purity, 99.79%) and olaparib ($C_{24}H_{23}FN_4O_3$; MW, 434.46; purity, 99.98%) were purchased from MedChemExpress (Princeton, NJ, USA). HPLC-grade acetonitrile and distilled water (Cat. Nos. 5-05-8 and 7732-18-5) were purchased from J.T. Baker (Phillipsburg, NJ, USA). Ammonium acetate was bought from Kanto Chemical (Tokyo, Japan). Other materials used were HPLC-grade or above.

Instrument and analytical methods

An API 4000 triple quadrupole mass spectrometer (AB Sciex, Framingham, MA, USA) fitted with an Agilent 1100 HPLC system (Agilent Technologies, Santa Clara, CA, USA) was used to analyze AZD5305 in ESI positive ion mode. A Synergi 4-μm Polar-RP 80-Å column (2.0×150 mm; Phenomenex, Torrance, CA, USA) kept at 40 °C was utilized to separate AZD5305 and olaparib (the internal standard; IS). Isocratic elution was performed using ammonium acetate (5 mM) in distilled water–acetonitrile (50:50, v/v) at a flow rate of 0.3 mL/min. The temperature of the autosampler was 10 °C. The mass spectrometer was used under the following operating conditions: ion spray voltage of 5500 V, curtain gas pressure of 20 psi, temperature of 600 °C, nebulizer gas pressure of 50 psi, and turbo gas pressure of 50 psi. The declustering potential, entry potential, collision energy, and collision cell exit potential of AZD5305 were 86, 10, 29, and 24 V, respectively, and those of the IS were 71, 10, 43, and 18 V, respectively. The simultaneous quantification of ion transitions at m/z 407.0 → 376.0 for AZD5305 and m/z 435.0 → 281.2 for the IS was accomplished using multiple reaction monitoring (MRM). The Analyst tool v.1.6.2 (AB Sciex, Framingham, MA, USA) was used to automatically combine the peak areas.

Sample preparation

To prepare working solutions (0.01–10 μg/mL), AZD5305 stock solution (1 mg/mL) was prepared in methanol and diluted using acetonitrile. Whole blood collected from the artery of six-week-old ICR mice was transferred to a heparin-coated tube and centrifuged to obtain blank mouse plasma. Stock and working solutions

and blank mouse plasma were stored at −20 °C until used for analysis. A standard sample was prepared using a tenfold concentration of the working solution. Standard samples with final concentrations of 1, 3, 10, 30, 100, 300, and 1000 ng/mL were prepared by adding 2 µL of each working solution to 18 µL blank mouse plasma and vortexing for 1 min. These samples were used to prepare the calibration curve for AZD5305.

A total of 160 µL acetonitrile and 20 µL IS in acetonitrile (300 ng/mL) were used for deproteinization. The plasma sample was vortexed and centrifuged at 13,500 rpm for 10 min, 100 µL supernatant was transferred to an analytical vial, and 5 µL was analyzed by LC–MS/MS. Quality control (QC) samples were prepared independently as the standard samples were prepared, with AZD5305 values of 1 ng/mL (LLOQ), 3 ng/mL (low QC; LQC), 30 ng/mL (middle QC; MQC), and 900 ng/mL (high QC; HQC).

Analytical method validation

According to the recommendations from the European Medicines Agency (EMA) and United States Food and Drug Administration (US FDA), specificity, selectivity, linearity, accuracy, precision, stability, matrix effect, recovery, process efficiency, and dilution integrity were validated to confirm reproducibility of the LC–MS/MS method for AZD5305 analysis in mice plasma (US FDA 2018; EMA 2011).

By comparing the peaks obtained for blank plasma samples from six ICR mice, specificity and selectivity were evaluated. Comparisons were made among the chromatograms of plasma samples taken an hour after dosing and samples of blank plasma, blank plasma spiked with the IS, and blank plasma spiked with AZD5305 and the IS. By comparing the peak forms and retention times of the analyte and the IS, the interference effects of endogenous substances in plasma were evaluated.

Linearity was assessed on the basis of correlation coefficient (r) of the calibration curve of AZD5305 in plasma over a standard range of 1–1000 ng/mL. An $r \geq 0.990$ was considered acceptable (Yoon et al. 2020). By plotting the ratio of analyte to IS peak area versus nominal concentration and fitting the data using least squares linear regression with a weighting value of $1/x^2$, the calibration curve was prepared (Gu et al. 2014).

Accuracy and precision were assessed using LLOQ, LQC, MQC, and HQC. Intraday and inter-day accuracy and precision were assessed by reiterating the experiment five times a day and for three consecutive days, respectively. Accuracy and precision values were determined as the relative error (%RE), and coefficient of variation (%CV), respectively, between the calculated and nominal concentrations. The criteria were ± 15% RE and ≤ 15% CV. The criterion for LLOQ data acceptance was within 20%.

The matrix effect, recovery, and process efficiency were assessed at all QC levels (LQC, MQC, and HQC; $n = 5$ for each level), where set 1 is peak areas of the spiked analyte and the IS in pure acetonitrile; set 2 is peak areas of the spiked analyte and the IS in extracted plasma; and set 3 is peak areas of the sample extract containing the analyte and the IS. The matrix effect, recovery, and process efficiency were calculated by dividing set 1 by set 2, set 2 by set 3, and set 1 by set 3, respectively (Choi et al. 2021).

Stability was evaluated using LQC and HQC under five different conditions: 2 and 4 weeks at −20 °C, three freeze–thaw cycles, 6 h at room temperature (25 °C), and pretreatment followed by 24 h in an autosampler at 10 °C.

Dilution integrity was examined to confirm that dilution of the sample did not influence the analysis. Test samples were prepared at 9 and 36 µg/mL [10 and 40 times more concentrated, respectively, than HQC (900 ng/mL)]. Dilution integrity was evaluated by calculating the %CV and %RE values of the samples following 10- and 40-fold dilution.

In vitro pharmacokinetics study

A microsomal stability test was performed using microsomes of mice, rats, dogs, and humans (BD Biosciences, Franklin Lakes, NJ, USA). A stock solution (10 mM) was prepared in methanol. Then, 25 µL of microsomes was added to 440 µL of phosphate-buffered saline (pH 7.4; 6.7 mM) and incubated in a water bath at 37 °C for approximately 5 min. After adding 5 µL AZD5305 solution (2 µM final concentration), a zero-time sample was collected and incubated with an NADPH regeneration system solution. Samples were obtained at 5, 15, 30, and 60 min, and the reaction was terminated using acetonitrile.

The fraction of bound AZD5305 in plasma was assessed using a plasma protein binding assay kit (rapid equilibrium dialysis, RED; Thermo Scientific, Waltham, MA, USA) (van Liempd et al. 2011). AZD5305 was added to the plasma of mice, rats, dogs, and humans to obtain a final concentration of 1 µg/mL. The plasma sample (200 µL) was put into the red chamber of a semipermeable membrane device, and 350 µL phosphate-buffered saline (pH 7.4; 6.7 mM) was added into the white chamber. After 4 h of incubation in a water bath (37 °C, 100 rpm), 50 µL each of the plasma and buffer samples was obtained and pretreated with the IS in acetonitrile (300 ng/mL). Plasma protein binding was calculated using the equation below (Ji et al. 2020).

$$Plasma\ protein\ binding = 1 - \frac{\text{buffer concentration}}{\text{plasma concentration}}$$

For the plasma stability assay, 10 µL AZD5305 in methanol (50 µg/mL) was added to 490 µL blank of each of mouse, rat, dog, and human plasma to achieve a final concentration of 1 µg/mL. Samples (50 µL) were obtained at 0, 0.25, 0.5, 1, and 2 h during incubation in a water bath (37 °C, 100 rpm). Each sample was deproteinized by adding acetonitrile containing the IS (300 ng/mL).

Application to pharmacokinetic studies

The pharmacokinetics of AZD5305 in mice were investigated using the newly developed and established LC–MS/MS assay. All animal experiments were acknowledged beforehand by the Institutional Animal Care and Use Committee of Chungnam National University (202203-CNU-056; Daejeon, Republic of Korea). ICR mice (26–33 g, male, six-week-old) were purchased from Orient Bio Inc. (Seongnam, Republic of Korea). A humidity level of 40–65% and a temperature range of 20–26 °C were maintained in the animal room. During the acclimation period, animals had free access to food and water, and fasting began 4 h before the animal experiment. Food and water were provided 4 h after drug administration. The dosing solution of AZD5305 was prepared by dissolving AZD5305 powder in dimethyl sulfoxide–polyethylene glycol and 400–0.1 N hydrochloric acid–phosphate-buffered saline (pH 7.4; 6.7 mM) (5:30:10:55, v/v/v/v). The dosing solution was applied to mice either orally (PO) using a gavage needle, at doses of 0.1, 0.3, 1, and 3 mg/kg, or as a single intravenous (IV) bolus into the tail vein at dosages of 0.1, 0.3, and 1 mg/kg. Using heparin-coated capillaries, whole blood (50 µL) was collected from the retro-orbital plexus at 0.083 (IV only), 0.25, 0.5, 1, 2, 4, 8 and 24 h after AZD5305 administration. To collect plasma (20 µL), whole blood was centrifuged at 13,500 rpm for 5 min. Plasma was kept at—20 °C until analysis. For analyzing plasma samples, 20 µL IS and 160 µL acetonitrile were added to 20 µL mouse plasma. For plasma samples that required dilution, the IS and acetonitrile were added after diluting 10 or 40 times using blank mouse plasma. The samples were vortexed and then centrifuged for 10 min at 13,500 rpm. Then, 100 µL supernatant was transferred to an analytical vial.

Pharmacokinetic parameters and statistical analysis

Pharmacokinetic parameters of AZD5305 in mice were assessed by non-compartmental analysis using Phoenix v.8.3 program (Certara L.P., Princeton, NJ, USA). The elimination rate constant (k_e), which is the rate at which a drug disappears in the elimination phase, was calculated using log-linear regression. The half-life ($t_{1/2}$), which is the time at which a drug is reduced by half in the elimination phase, was calculated by dividing natural logarithm of 2 by k_e values. The area under the curve from zero to infinity (AUC_{inf}) represents the level of drug exposure in the body, and was calculated using the trapezoidal rule and standard area extrapolation methods (Kim et al. 2015).

All data are presented as mean ± standard deviation (SD). The pharmacokinetic parameters were statistically analyzed using one-way analysis of variance (ANOVA) with Prism v.9.4.1 (GraphPad Software, San Diego, CA, USA). Statistical significance was set at $p < 0.05$.

Results and discussion

LC–MS/MS method development

In the positive ion mode, AZD5305 and the IS produced protonated ions ($[M+H]^+$) at 407.0 and 435.0, respectively. Detection was conducted using triple quadrupole mass spectrometry with MRM transitions at m/z 407.0 → 376.0 for AZD5305 and m/z 435.0 → 281.2 for the IS. For AZD5305, the product ion corresponding to m/z 407.0 → 187.0 showed higher sensitivity than the selected product ion, but the background noise was more severe. Therefore, m/z 407.0 → 376.0 was selected for AZD5305 determination (Fig. 1).

Chromatographic separation was conducted using different columns, mobile phases, and elution modes to optimize peak shape, symmetry, and retention time. Formic acid in distilled water and acetonitrile, which are commonly used in electrospray ionization LC–MS/MS, typically provide high sensitivity (Churchwell et al. 2005). However, owing to insufficient interactions with the columns (C18, C8, and phenyl), it had a very fast retention time (< 0.6 min), accompanied by peak broadening or high background noise. Furthermore, ion suppression by polyethylene glycol 400 (PEG400), an excipient in the AZD5305 dosing solution, was highly severe (Larger et al. 2005). When ammonium formate in distilled water (10 mM) and acetonitrile were used, the retention times of the IS and AZD5305 differed significantly for each column, and the effect of PEG remained severe. In addition, distorted peaks owing to noise were observed at low concentrations. Among the investigated conditions, a Phenomenex 4-µm Polar-RP 80-Å column (2.0 × 150 mm) with ammonium acetate in distilled water (5 mM)–acetonitrile (50:50, v/v) provided AZD5305 peaks with the highest intensity and symmetry (Fig. 2). Under the optimal conditions, the retention times of AZD5305 and IS were 1.82 min and 1.99 min, respectively. Furthermore, to avoid contamination of the instrument by the matrix, a needle clean-up step was carried out using 50% methanol before and after sample injection. No noticeable changes in retention time, intensity, peak shape, background

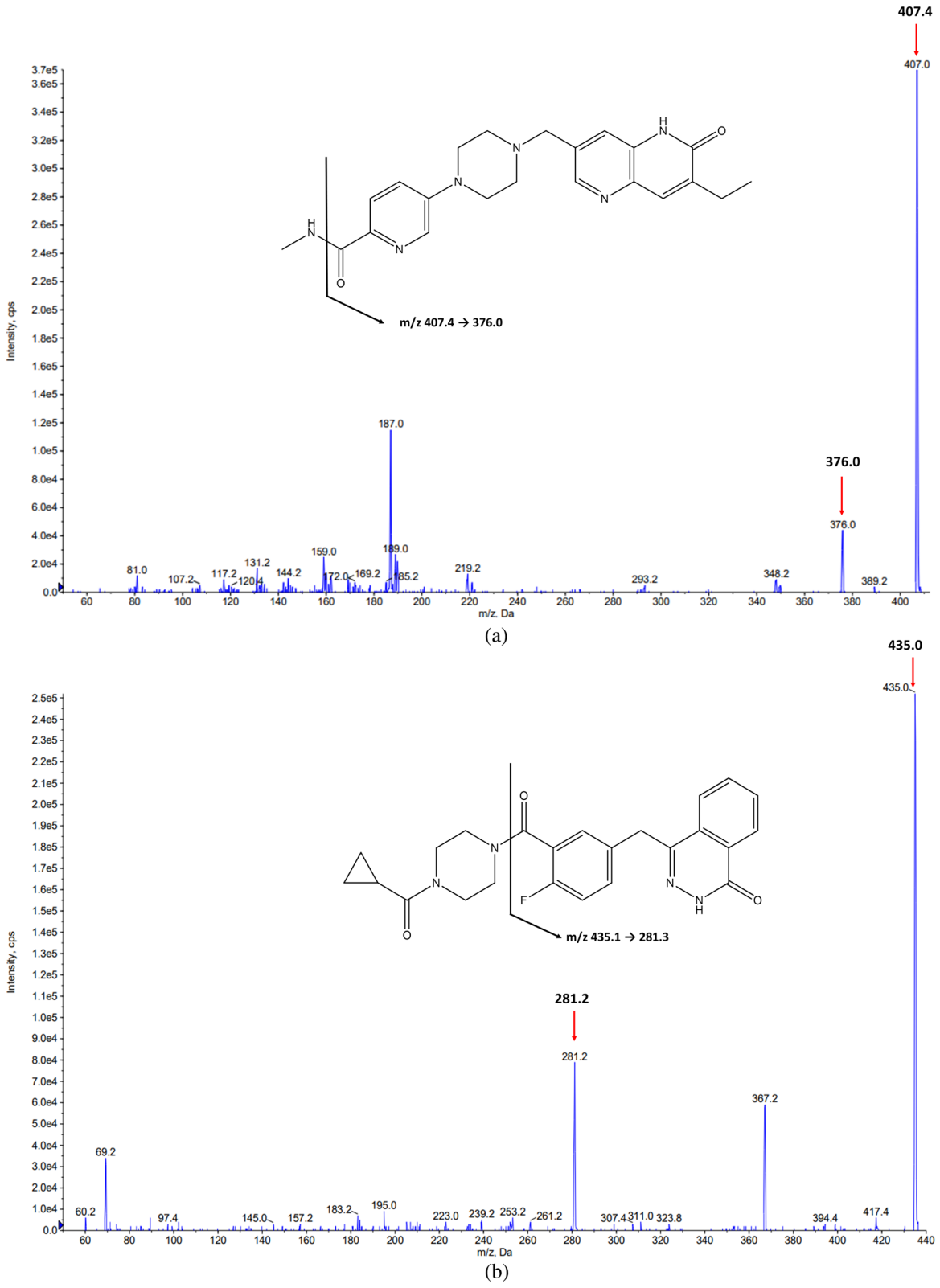

Fig. 1 Product ion mass spectra of **a** AZD5305 and **b** olaparib

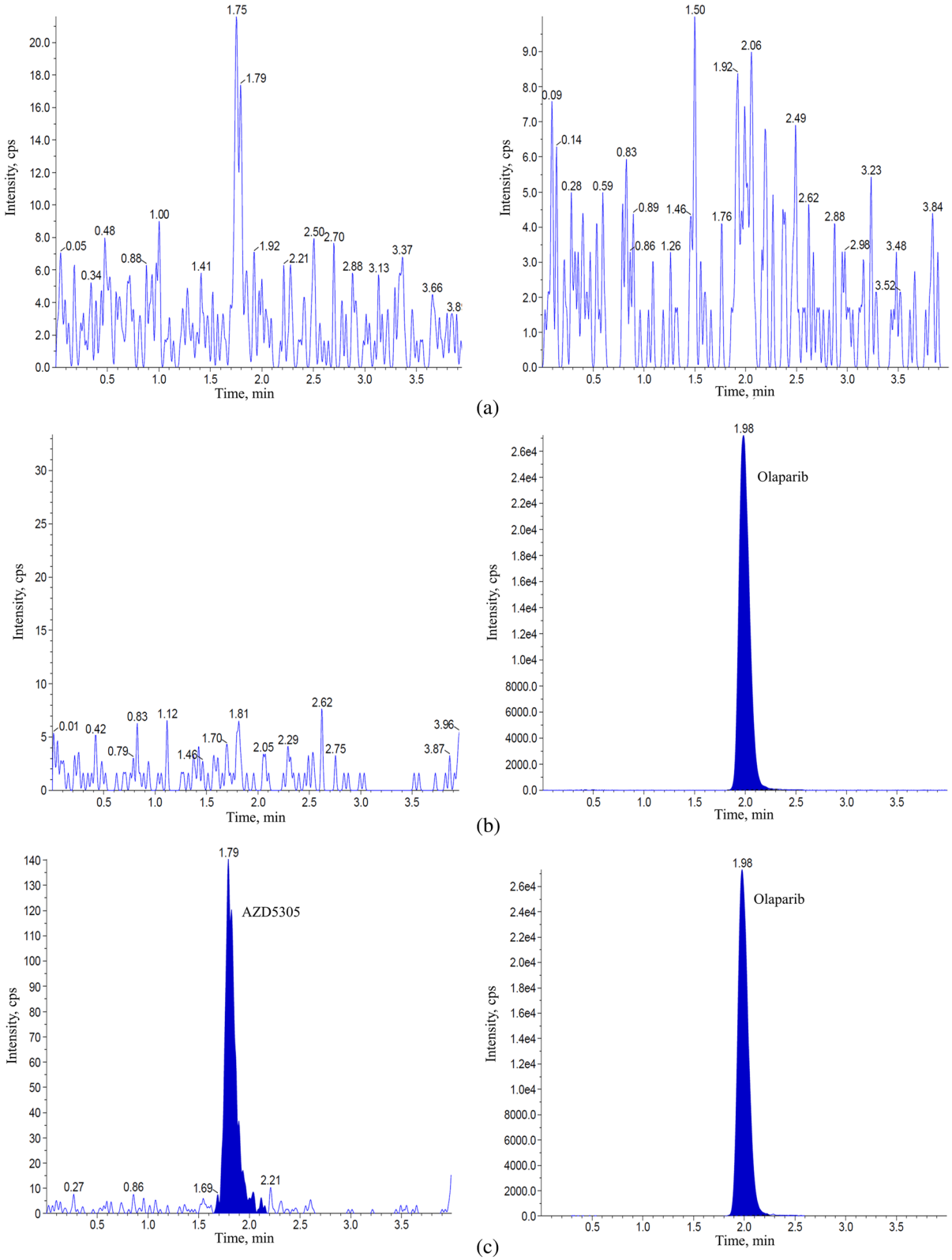

Fig. 2 LC–MS/MS chromatograms of AZD5305 (left) and olaparib (right): **a** after deproteinization of blank mice plasma, **b** zero sample, **c** LLOQ, and **d** 1 h after PO administration of AZD5305 at a dose of 1 mg/kg in mice

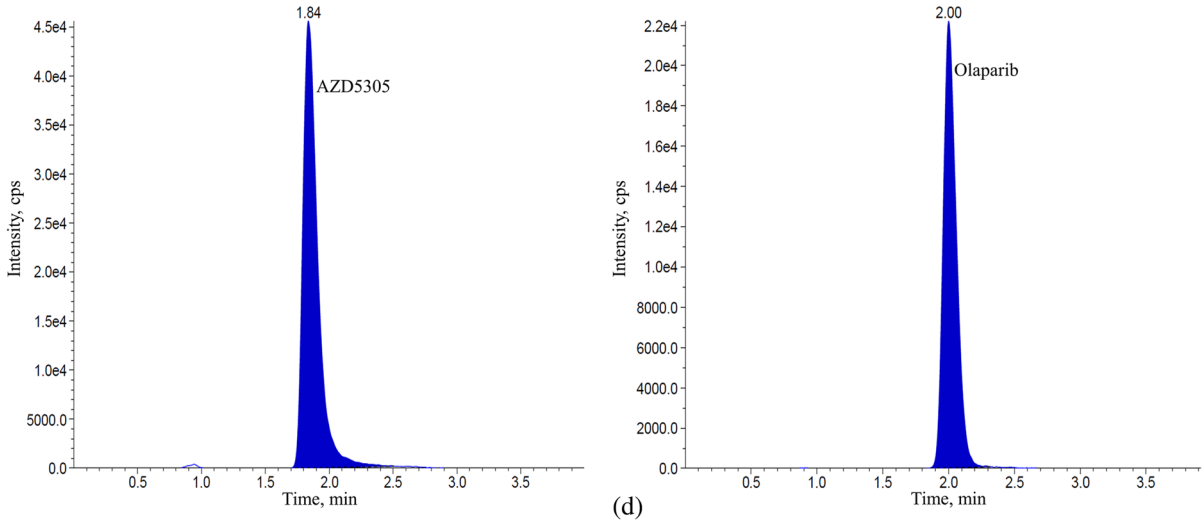

Fig. 2 continued

noise, and contamination occurred following analyses of several AZD5305 plasma samples. Biological samples are often prepared for analysis using solid-phase extraction, liquid–liquid extraction, or protein precipitation using organic solvents (Kishikawa et al. 2019). Protein precipitation using organic solvents, such as acetonitrile, removes endogenous proteins from biological samples resulting in high recovery rates. In addition, this approach is convenient and fast, allowing the pretreatment of a large number of biological samples. Therefore, protein precipitation using acetonitrile was applied in this analysis.

Method validation

When mouse plasma was pretreated with acetonitrile for protein precipitation, no interference of endogenous substances was observed during analysis (Fig. 2). The signal-to-noise ratio was > 5; therefore, the LLOQ was set at 1 ng/mL. The retention times of AZD5305 and the IS were 1.82 and 1.99 min, respectively. When using the optimized LC–MS/MS analysis method, it showed sufficient specificity.

The accuracy and precision of AZD5305 assay were assessed at the LLOQ and QC levels (1, 3, 30, and 900 ng/mL) using %RE and %CV (Table 1). Intraday and inter-day precision values in mouse plasma were 7.24 and 10.1%, respectively, whereas intraday and inter-day accuracy values were 8.94 and 3.24%, respectively. Results under 20% for the LLOQ and 15% for other concentrations indicated reproducibility and reliability of the AZD5305 assay in mouse plasma.

The stability of AZD5305 in mouse plasma was assessed by analyzing QC samples (LQC and HQC) under different storage conditions (Table 2). AZD5305 was stable at − 20 °C for up to 4 weeks, over three freeze–thaw cycles, at room temperature (25 °C) for 6 h, and in an autosampler at 10 °C for 24 h.

Table 1 Intra- and inter-day accuracy and precision of the LC–MS/MS method

Nominal concentration (ng/mL)	Measured concentration (ng/mL)	Accuracy (%RE)	Precision (%CV)
Mouse plasma			
Intra-day (n = 5)			
1	1.01 ± 0.0615	0.917	6.09
3	2.91 ± 0.178	3.06	6.12
30	27.3 ± 0.917	8.94	3.36
900	828 ± 59.9	8.00	7.24
Inter-day (n = 15)			
1	1.00 ± 0.101	0.172	10.1
3	2.90 ± 0.240	3.24	8.26
30	29.2 ± 2.03	2.78	6.94
900	904 ± 85.6	0.444	9.47

Matrix effect, recovery, and process efficiency of AZD5305 were confirmed at all QC levels (3, 30 and 900 ng/mL) (Table 3). The values for each of the three items were 86.5–96.5, 87.1–99.7, and 84.0–86.8%, respectively, and the IS values were 94.6, 98.3, and 90.4%, respectively. The CV of matrix effect was < 15%. These results indicate that using an organic solvent for deproteinization is a fast and efficient method for extracting AZD5305 from mouse plasma.

Table 2 Stability of AZD5305 in mice plasma (mean ± SD, $n = 5$)

Storage conditions	Nominal concentration (ng/mL)	Stability (%)
Processed sample (autosampler, 10 °C, 24 h)	3	95.1 ± 5.22
	900	98.9 ± 5.71
Long-term (2 weeks at − 20 °C)	3	96.9 ± 4.73
	900	96.8 ± 1.82
Long-term (4 weeks at − 20 °C)	3	97.5 ± 2.54
	900	98.9 ± 3.92
Freeze–thaw (3 cycles, − 20 °C ⟶ RT)	3	96.6 ± 9.10
	900	99.7 ± 2.69
6 h after room temperature (25 °C)	3	99.1 ± 4.37
	900	98.5 ± 1.40

The dilution integrity was 3.21 and 2.83 for precision (%CV) and accuracy values (%RE), respectively, at a dilution factor of 10, and 3.88 and 0.630 at a dilution factor of 40, respectively.

In vitro pharmacokinetic study

Microsomal stability was tested using the microsomes of mice, rats, dogs, and humans. As shown in Fig. 3a, the amounts of AZD5305 remaining in the microsomes of mice, rats, dogs, and humans were 97.6 ± 14.8, 97.5 ± 2.52, 98.0 ± 6.94, and 102 ± 6.14%, respectively. Therefore, AZD5305 was highly stable in the microsomes of these species.

Plasma stability tests were conducted using the plasma of mice, rats, dogs, and humans. The amounts of AZD5305 remaining in the plasma of mice, rats, dogs, and humans were 100 ± 5.16, 106 ± 3.16, 98.8 ± 12.6, and 97.6 ± 2.36%, respectively (Fig. 3b). Overall, AZD5305 was highly stable in the plasma of mice, rats, dogs, and humans and did not dissipate over an incubation time of 120 min.

The plasma protein binding rate was assessed using an equilibrium dialysis kit. At a dose of 1 μg/mL AZD5305, the binding fractions in plasma of mice, rats, dogs, and humans were 83.2 ± 0.829, 95.1 ± 0.935, 96.2 ± 0.281, and 96.6 ± 0.371%, respectively. These results suggested that AZD5305 had a high affinity for plasma proteins of all the species except mice.

In vivo pharmacokinetics study

Pharmacokinetic investigation in mice was conducted using the established LC–MS/MS assay. The temporal profiles following IV bolus injection at doses of 0.1–1 mg/kg AZD5305 are displayed in Fig. 4a, and the corresponding pharmacokinetic parameters are summarized in Table 4a. In the concentration–time profiles after IV administration, AZD5305 showed a biexponential decline with distinct distribution and elimination phases. The slope of the elimination phase was constant, even when the dose was increased from 0.1 to 1 mg/kg. In addition, $t_{1/2}$ values were not significantly different according to dose (5.96 ± 0.589, 5.86 ± 0.873, and 5.99 ± 0.459 h for doses of 0.1, 0.3, and 1 mg/kg, respectively). The total systemic clearance (CL) values were 17.9 ± 1.94, 15.5 ± 1.65, and 15.2 ± 0.724 mL/h/kg for doses of 0.1, 0.3, and 1 mg/kg, respectively. These CL values were very low with respect to blood flow rate in the liver of mice (5400 mL/h/kg) (Nguyen et al. 2022). The steady state volume of distribution (V_{ss}) values were 135 ± 6.89, 116 ± 10.3, and 115 ± 11.1 mL/kg for doses of 0.1, 0.3, and 1 mg/kg, respectively. The volume of distribution was less than the volume of extracellular fluid in mice, indicating that AZD5305 had a limited distribution. CL and V_{ss} values also showed no significant differences according to doses. The maximum concentration (C_{max}) values for 0.3 and 1 mg/kg doses were 3.09 and 8.93 times higher, respectively, than that for a dose of 0.1 mg/kg. In addition, the AUC_{inf} values at 0.3 and 1 mg/kg were 3.61 and 11.7 times higher, respectively, than that for a dose of 0.1 mg/kg. The dose normalized C_{max}, AUC_{inf}, and AUC_{last} values did not show significant differences ($p > 0.05$, one-way ANOVA). Pharmacokinetic parameters (CL, V_{ss}, and $t_{1/2}$) were consistent across doses in the range of 0.1–1 mg/kg, and AZD5305 exhibited dose-independent pharmacokinetics, suggesting no saturation patterns in distribution and metabolism/excretion. Drugs exhibiting

Table 3 Matrix effect, recovery, and process efficiency of AZD5305 (mean ± SD, $n = 5$)

Nominal concentration (ng/mL)	Matrix effect (%)	Recovery (%)	Process efficiency (%)
Mouse plasma			
AZD5305			
3	96.5 ± 3.43	87.1 ± 9.59	84.0 ± 3.43
30	86.5 ± 0.906	99.5 ± 3.27	86.0 ± 0.906
900	87.1 ± 1.29	99.7 ± 1.79	86.8 ± 1.29
Olaparib (IS, 300 ng/mL)	94.6 ± 5.15	98.3 ± 4.83	90.4 ± 4.19

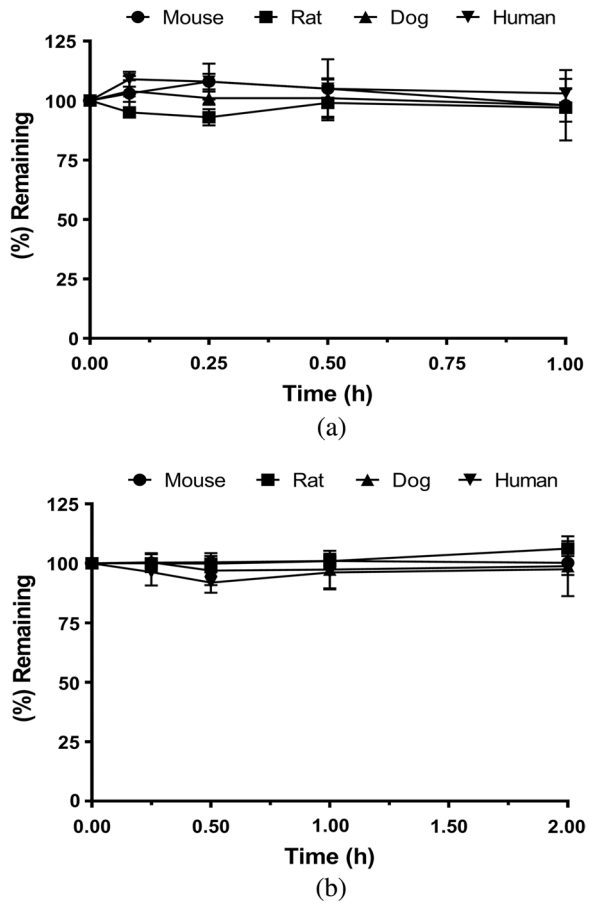

Fig. 3 **a** Microsomal stability and **b** plasma stability of AZD5305 (mean ± SD, *n* = 4)

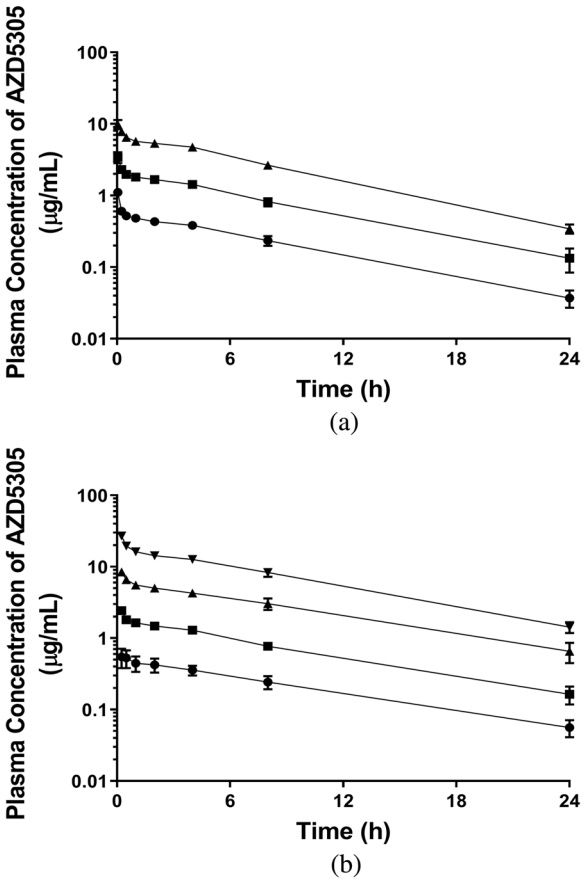

Fig. 4 Plasma concentration–time curves of AZD5305 after **a** a single IV bolus injection in fasted ICR mice (●: 0.1 mg/kg, ■: 0.3 mg/kg, ▲: 1 mg/kg) and **b** a single oral administration in fasted ICR mice (●: 0.1 mg/kg, ■: 0.3 mg/kg, ▲: 1 mg/kg, ▼: 3 mg/kg) (mean ± SD, *n* = 5)

such dose-independent pharmacokinetic characteristics show strength in terms of easy prediction of drug efficacy and toxicity because the dose and drug exposure are proportional.

The temporal profiles after a single oral administration at doses between 0.1 and 3 mg/kg in mice are shown in Fig. 4b, and the corresponding pharmacokinetic parameters are summarized in Table 4b. In the concentration–time profiles after oral administration, the maximum AZD5305 concentration was rapidly achieved followed by a biexponential decline. The time of peak plasma concentration (T_{max}) values were 0.300 ± 0.112, 0.250 ± 0.000, 0.250 ± 0.000, and 0.250 ± 0.000 h at 0.1, 0.3, 1, and 3 mg/kg, respectively, indicating that AZD5305 was rapidly absorbed. At 0.1, 0.3, 1, and 3 mg/kg, the C_{max} values were 0.555 ± 0.166, 2.42 ± 0.287, 8.46 ± 0.867, and 26.9 ± 2.38 μg/mL, respectively; the $t_{1/2}$ values were 7.67 ± 1.50, 6.85 ± 0.920, 7.32 ± 1.11, and 6.37 ± 0.695 h, respectively; and the AUC_{inf} values were 5.89 ± 1.02, 19.3 ± 2.03, 71.9 ± 9.76, and 192 ± 16.8 μg h/mL, respectively. The exposure level of AZD5305 in mice was significantly higher than that of common oral drugs, which can be attributed to its remarkably high metabolic stability and low volume of distribution. In a xenograft model, the administration of AZD5305 at a dose of 0.1 mg/kg demonstrated similar effects to those of olaparib at a dose of 100 mg/kg (Illuzzi et al. 2021). When normalized by dose, the exposure level of AZD5305 was approximately 300 times higher than that of olaparib (AZD5305: AUC 192 μg·h/mL at 3 mg/kg vs. olaparib: AUC 38.6 μmol h/L at 80 mg/kg) (CDER 2014). This significant difference in exposure levels is considered to be the primary factor contributing to the observed disparity in their antitumor effects.

T_{max}, $t_{1/2}$, normalized C_{max}, and normalized AUC_{inf} values did not significantly differ in the oral administration group ($p > 0.05$). The bioavailability (F%) values were 104, 94.7, and 108% for the PO groups at 0.1–1.0 mg/kg, respectively. The F% value for oral administration at 3 mg/kg was 97.4%, which corresponded to the IV injection group at 1 mg/kg, suggesting that AZD5305 was

Table 4 Pharmacokinetic parameters of AZD5305 after IV injection and oral gavage administration

Parameters	Dose		
	0.1 mg/kg	**0.3 mg/kg**	**1 mg/kg**
a Intravenous bolus injection to ICR mice			
T_{max} (h)	0.0500 ± 0.000	0.0500 ± 0.000	0.0500 ± 0.000
C_{max} (μg/mL)	1.11 ± 0.133	3.42 ± 0.580	9.88 ± 1.44
$t_{1/2}$ (h)	5.97 ± 0.589	5.86 ± 0.873	5.99 ± 0.459
AUC_{last} (μg·h/mL)	5.30 ± 0.502	19.2 ± 2.12	62.1 ± 3.46
AUC_{inf} (μg·h/mL)	5.63 ± 0.615	20.4 ± 2.60	66.0 ± 3.23
MRT (h)	7.60 ± 0.820	7.60 ± 1.10	7.63 ± 0.522
CL (mL/h/kg)	17.9 ± 1.94	15.5 ± 1.65	15.2 ± 0.724
V_{ss} (mL/kg)	135 ± 6.89	117 ± 10.3	116 ± 11.1

Parameters	Dose			
	0.1 mg/kg	**0.3 mg/kg**	**1 mg/kg**	**3 mg/kg**
b Oral gavage administration to ICR mice				
T_{max} (h)	0.300 ± 0.112	0.250 ± 0.000	0.250 ± 0.000	0.250 ± 0.000
C_{max} (μg/mL)	0.555 ± 0.166	2.42 ± 0.287	8.46 ± 0.867	26.9 ± 2.38
$t_{1/2}$ (h)	7.67 ± 1.50	6.85 ± 0.920	7.32 ± 1.11	6.37 ± 0.695
AUC_{last} (μg·h/mL)	5.25 ± 0.981	17.6 ± 1.46	64.7 ± 6.95	179 ± 15.7
AUC_{inf} (μg·h/mL)	5.89 ± 1.02	19.3 ± 2.03	71.9 ± 9.76	193 ± 16.8
MRT (h)	10.1 ± 2.22	8.82 ± 1.17	9.48 ± 1.55	8.23 ± 0.692
F (%)	105 ± 18.0	94.8 ± 9.96	.109 ± 14.8	97.4 ± 8.48

Data are shown as means ± SD (n = 5)

rapidly and completely absorbed and underwent minimum hepatic first-pass effects. For different IV and PO doses, bioavailability may exceed 100% due to saturation of elimination processes (e.g., saturation of metabolic enzymes). However, metabolic saturation does not appear to have occurred since AZD5305 showed linear pharmacokinetics with increasing dose. Therefore, the fact that the bioavailability exceeded 100% with some doses is considered to be due to differences between mice. Drugs with high bioavailability have the advantage of high exposure following minimal administration compared to molecules that have low bioavailability and thus low individual differences. These data are consistent with the results of the microsomal stability test that indicated high stability of AZD5305 to phase 1 metabolic mechanisms such as cytochrome P450 metabolism. This finding indicates that the absorption, distribution, and elimination processes of AZD5305 follow linear pharmacokinetics over the experimental dose range (0.1–3 mg/kg).

Conclusion

The purpose of our study was to develop a sensitive and selective LC–MS/MS analysis method for AZD5305 to elucidate its limited known pharmacokinetic characteristics. The reliability and reproducibility of the analysis method were verified according to the FDA and EMA guidelines, and it was successfully applied to pharmacokinetic studies. Overall, the pharmacokinetic parameters for AZD5305 in mice were determined. To summarize the results, AZD5305 showed very high C_{max}, and AUC $_{inf}$ values and very low CL and V_{ss} values compared to the orally administered dose. In addition, it was very stable in microsomes and showed a very high bioavailability of close to 100%. However, further studies are needed on the tissue distribution and excretion of AZD5305. Additionally, since it was very stable to Phase 1 metabolic processes, studies related to the Phase 2 metabolism are also needed. Our results can provide insights into the pharmacological properties of AZD5305 and aid in developing more effective PARP inhibitors for treating cancers associated with BRCA mutations.

Abbreviations

BCSG	Breast Cancer Susceptibility Gene
CYP	Cytochrome P450
DSBs	Double-Strand Breaks
IS	Internal Standard
IV	Intravenous
LC-MS/MS	Liquid chromatography with tandem mass spectroscopy
LLOQ	Lower Limit of Quantification
MRM	Multiple Reaction Monitoring
PARP	Poly (ADP-ribose) polymerase

PEG400	Polyethylene Glycol 400
PO	Per Oral
QC	Quality control

Acknowledgements
Not applicable.

Author contributions
GJL: formal analysis, methodology, research, writing—original draft, visualization, data curation; JWK: formal analysis, validation, methodology, research, visualization, data curation; HIC: methodology, validation, research, data curation; JYC: methodology, validation, research, data curation; KHC: methodology, writing—review & editing; TSK: conceptualization, writing—review & editing, supervision, project administration, funding acquisition.

Funding
This work was supported by the Chungnam National University and the National Research Foundation of Korea (Grant Number 21R1F1A1062551).

Availability of data and materials
The data that support the findings of this study are available from the corresponding author on reasonable request.

Declarations

Ethics approval and consent to participate
Not applicable.

Consent for publication
Not applicable.

Competing interests
The authors declare that they have no known competing financial interests or personal relationships that could have appeared to influence the work reported in this paper.

Author details
[1]Graduate School of New Drug Discovery and Development, Chungnam National University, 99 Daehak-ro, Yuseong-gu, Daejeon 34134, Republic of Korea. [2]College of Pharmacy and Inje Institute of Pharmaceutical Sciences and Research, Inje University, 197 Inje-ro, Gimhae 50834, Republic of Korea.

Received: 9 May 2023 Accepted: 25 July 2023
Published online: 09 August 2023

References

Armstrong N, Ryder S, Forbes C, Ross J, Quek RG. A systematic review of the international prevalence of BRCA mutation in breast cancer. Clin Epidemiol. 2019. https://doi.org/10.2147/CLEP.S206949.

Bruin MAC, Sonke GS, Beijnen JH, Huitema ADR. Pharmacokinetics and pharmacodynamics of PARP inhibitors in oncology. Clin Pharmacokinet. 2022;61(12):1649–75. https://doi.org/10.1007/s40262-022-01167-6.

Center for drug evaluation and research. pharmacology review(s): LYNPARZA (olaparib). 2014, https://www.accessdata.fda.gov/drugsatfda_docs/nda/2014/206162Orig1s000PharmR.pdf. Accessed 20 June 2023.

Chen A. PARP inhibitors: its role in treatment of cancer. Chin J Cancer. 2011;30(7):463–71. https://doi.org/10.5732/cjc.011.10111.

Choi HI, Kim T, Lee SW, Kim JW, Noh YJ, Kim GY, Park HJ, Chae YJ, Lee KR, Kim SJ, Koo TS. Bioanalysis of niclosamide in plasma using liquid chromatography-tandem mass and application to pharmacokinetics in rats and dogs. J Chromatogr B Analyt Technol Biomed Life Sci. 2021;1179:122862. https://doi.org/10.1016/j.jchromb.2021.122862.

Churchwell MI, Twaddle NC, Meeker LR, Doerge DR. Improving LC-MS sensitivity through increases in chromatographic performance: comparisons of UPLC-ES/MS/MS to HPLC-ES/MS/MS. J Chromatogr B Analyt Technol Biomed Life Sci. 2005;825(2):134–43. https://doi.org/10.1016/j.jchromb.2005.05.037.

Dziadkowiec KN, Gasiorowska E, Nowak-Markwitz E, Jankowska A. PARP inhibitors: review of mechanisms of action and BRCA1/2 mutation targeting. Prz Menopauzalny. 2016;15(4):215–9. https://doi.org/10.5114/pm.2016.65667.

EMA Guideline on bioanalytical method validation (2011). https://www.ema.europa.eu/en/documents/scientific-guideline/guideline-bioanalytical-method-validation_en.pdf. Accessed 13 Feb 2023

Gu H, Liu G, Wang J, Aubry AF, Arnold ME. Selecting the correct weighting factors for linear and quadratic calibration curves with least-squares regression algorithm in bioanalytical LC-MS/MS assays and impacts of using incorrect weighting factors on curve stability, data quality, and assay performance. Anal Chem. 2014;86(18):8959–66. https://doi.org/10.1021/ac5018265.

Illuzzi G, Staniszewska AD, Gill SJ, Pike A, McWilliams L, Critchlow SE, Cronin A, Fawell S, Hawthorne G, Jamal K, Johannes J, Leonard E, Macdonald R, Maglennon G, Nikkilä J, O'Connor MJ, Smith A, Southgate H, Wilson J, Leo E. Preclinical characterization of AZD5305, a next-generation, highly selective PARP1 inhibitor and trapper. Clin Cancer Res. 2021;28(21):4724–36. https://doi.org/10.1158/1078-0432.Ccr-22-0301.

Ji YG, Shin YM, Jeong JW, Choi HI, Lee SW, Lee JH, Lee KR, Koo TS. Determination of motolimod concentration in rat plasma by liquid chromatography-tandem mass spectrometry and its application in a pharmacokinetic study. J Pharm Biomed Anal. 2020;179:112987. https://doi.org/10.1016/j.jpba.2019.112987.

Johannes JW, Balazs A, Barratt D, Bista M, Chuba MD, Cosulich S, Critchlow SE, Degorce SL, Di Fruscia P, Edmondson SD, Embrey K, Fawell S, Ghosh A, Gill SJ, Gunnarsson A, Hande SM, Heightman TD, Hemsley P, Illuzzi G, Lane J, Larner C, Leo E, Liu L, Madin A, Martin S, McWilliams L, O'Connor MJ, Orme JP, Pachl F, Packer MJ, Pei X, Pike A, Schimpl M, She H, Staniszewska AD, Talbot V, Underwood E, Varnes JG, Xue L, Yao T, Zhang K, Zhang AX, Zheng X. Discovery of 5-{4-[(7-ethyl-6-oxo-5, 6-dihydro-1, 5-naphthyridin-3-yl) methyl] piperazin-1-yl}-N-methylpyridine-2-carboxamide (AZD5305): a PARP1–DNA trapper with high selectivity for PARP1 over PARP2 and other PARPs. J Med Chem. 2021;64(19):14498–512. https://doi.org/10.1021/acs.jmedchem.1c01012.

Kim TH, Jeong JW, Song JH, Lee KR, Ahn S, Ahn SH, Kim S, Koo TS. Pharmacokinetics of enzalutamide, an anti-prostate cancer drug, in rats. Arch Pharm Res. 2015;38(11):2076–82. https://doi.org/10.1007/s12272-015-0592-9.

Kishikawa N, El-Maghrabey MH, Kuroda N. Chromatographic methods and sample pretreatment techniques for aldehydes determination in biological, food, and environmental samples. J Pharm Biomed Anal. 2019;175:112782. https://doi.org/10.1016/j.jpba.2019.112782.

Langelier MF, Lin X, Zha S, Pascal JM. Clinical PARP inhibitors allosterically induce PARP2 retention on DNA. Sci Adv. 2023;9(12):eadf7175. https://doi.org/10.1126/sciadv.adf7175.

Larger PJ, Breda M, Fraier D, Hughes H, James CA. Ion-suppression effects in liquid chromatography–tandem mass spectrometry due to a formulation agent, a case study in drug discovery bioanalysis. J Pharm Biomed Anal. 2005;39(1–2):206–16. https://doi.org/10.1016/j.jpba.2005.03.009.

Lee J, Ledermann J, Kohn E. PARP Inhibitors for BRCA1/2 mutation-associated and BRCA-like malignancies. Ann Oncol. 2014;25(1):32–40.

Mateo J, Lord CJ, Serra V, Tutt A, Balmana J, Castroviejo-Bermejo M, Cruz C, Oaknin A, Kaye SB, de Bono JS. A decade of clinical development of PARP inhibitors in perspective. Ann Oncol. 2019;30(9):1437–47. https://doi.org/10.1093/annonc/mdz192.

Murai J, Huang SY, Das BB, Renaud A, Zhang Y, Doroshow JH, Ji J, Takeda S, Pommier Y. Trapping of PARP1 and PARP2 by clinical PARP inhibitors. Cancer Res. 2012;72(21):5588–99. https://doi.org/10.1158/0008-5472.CAN-12-2753.

Nguyen TT, Kim JW, Choi HI, Maeng HJ, Koo TS. Development of an LC-MS/MS method for ARV-110, a PROTAC molecule, and applications to pharmacokinetic studies. Molecules. 2022;27(6):1977. https://doi.org/10.3390/molecules27061977.

United States National Institutes of Health: National Library of Medicine Clinical Trials gov. https://clinicaltrials.gov/ct2/results?cond=&term=azd5305&cntry=&state=&city=. Accessed 20 March 2023

US FDA Guidance for Industry: bioanalytical method validation (2018). http://www.fda.gov/Drugs/GuidanceComplianceRegulatoryInformation/Guidances/default.htm. Accessed 20 Feb 2023

van Liempd S, Morrison D, Sysmans L, Nelis P, Mortishire-Smith R. Development and validation of a higher-throughput equilibrium dialysis assay for

plasma protein binding. J Lab Autom. 2011;16(1):56–67. https://doi.org/10.1016/j.jala.2010.06.002.
Yoon JH, Nguyen TT, Duong VA, Chun KH, Maeng HJ. Determination of KD025 (SLx-2119), a selective ROCK2 inhibitor, in rat plasma by high-performance liquid chromatography-tandem mass spectrometry and its pharmacokinetic application. Molecules. 2020;25(6):1369. https://doi.org/10.3390/molecules25061369.

Publisher's Note